

# Localized and Cellular Patterns in a Vibrated Granular Layer

Lev S.Tsimring<sup>1</sup> and Igor S. Aranson<sup>2,3</sup>

<sup>1</sup>*Institute for Nonlinear Science, University of California, San Diego, La Jolla, CA 92093-0402*

<sup>2</sup>*Bar Ilan University, Ramat Gan 52900, Israel*

<sup>3</sup>*Argonne National Laboratory, 9700 South Cass Avenue, Argonne, IL 60439*

(October 30, 2018)

We propose a phenomenological model for pattern formation in a vertically vibrated layer of granular material. This model exhibits a variety of stable cellular patterns including standing rolls and squares as well as localized objects (*oscillons* and *worms*), similar to recent experimental observations (Umbanhowar et al., 1996). The model is an amplitude equation for the parametrical instability coupled to the mass conservation law. The structure and dynamics of the solutions resemble closely the properties of localized and cellular patterns observed in the experiments.

PACS: 47.54.+r, 47.35.+i

Granular materials exhibit a unique mixture of properties of both liquids and solids [1]. Intensive theoretical, numerical and experimental studies of granular systems revealed a wide variety of new phenomena typical for granular systems, such as clustering and inelastic collapse [2], random force chains [3], granular convection [4] and cellular patterns in vibrated layers [5–7]. The very complicated rheology of granular media makes their theoretical analysis extremely difficult. Unlike fluid dynamics, there is no reliable continuum description of a granular system applicable in a wide range of conditions. The widely used approach is a straightforward simulation of many interacting particles in a gravity field [8,9].

Vibrated granular systems often manifest fluid-like behavior which resembles similar phenomena in conventional liquids. Recent experimental studies of vertically vibrated granular systems [5–7] demonstrated a rich variety of collective behavior ranging from standing waves, hexagons, squares to localized objects (particle-like *oscillons* [6] and one-dimensional *worms*, see [1]). Cellular patterns are remarkably similar to Faraday waves in fluids [10] which have recently been a subject of intensive research (see, e.g. [11]). The difference, however, is that the primary bifurcation to square patterns and *oscillons* is hysteretic: patterns disappear at less magnitude of the plate vibrations than they first appear. The localized objects, oscillating at half the frequency of plate vibrations  $\Omega/2$  on the background of a flat surface oscillating at  $\Omega$ , are observed in slightly subcritical parameter region for cellular patterns. Although some features of collective behavior of vibrated granular systems were reproduced in simulations of a large ensemble of inelastically interacting particles [9], the macroscopic understanding of the dynamics is lacking. In this Letter we propose a simple continuum model exhibiting phenomenology remarkably similar to the experimental observations. Due to its simplicity, it is amenable to a comprehensive analysis. Although this model is not derived from the corresponding microscopic equations of granular systems, it is instruc-

tive for interpretation of experimental data and may yield testable predictions.

The model consists of an amplitude equation for the order parameter  $\psi$  coupled to a conservation law for an average mass of granular material per unit area (or a local averaged thickness of the layer):

$$\partial_t \psi = \gamma \psi^* - (1 - i\omega)\psi + (1 + ib)\nabla^2 \psi - |\psi|^2 \psi - \rho \psi \quad (1)$$

$$\partial_t \rho = \alpha \nabla \cdot (\rho \nabla |\psi|^2) + \beta \nabla^2 \rho \quad (2)$$

Eq.(1) without the last term is a popular model for the parametric instability in oscillating liquid layer (see [13,14]). The order parameter  $\psi(x, y, t)$  characterizes local complex amplitude of the particle oscillations at the frequency  $\omega = \Omega/2$ . Linear terms in this equation can be derived from the dispersion relation for parametrically driven granular waves, expanded near frequency  $\omega$  and corresponding wavenumber  $k$  (here  $k = \sqrt{\omega/b}$ , parameter  $b$  must be chosen to reproduce the correct wavenumber at a given frequency). The term  $\gamma \psi^*$  provides parametric driving and leads to the excitation of standing waves. The term  $|\psi|^2 \psi$  phenomenologically accounts for the nonlinear saturation of oscillations provided in granular materials by restitution. The last term in Eq.(1) accounts for the coupling of the order parameter to the local average density  $\rho$ . As it is observed experimentally [5,6], the threshold value of the vibration amplitude  $\gamma$  for the parametric instability depends on the mean layer thickness [5] due to an increase of internal energy dissipation in thicker layers. Although one should generally expect this term to be  $f(\rho)\psi$  with  $f(\rho)$  saturating at large  $\rho$  (when the thickness of the layer is larger than the scale of typical perturbations), we hereafter limit ourselves with the simplest form  $f(\rho) = \rho$  corresponding to relatively thin layers (proportionality constant can be omitted after appropriate scaling of  $\rho$ ).

Eq.(2) describes the conservation of the granular material where  $\rho$  is a mass of granular material per unit square averaged over period of vibrations. Two different physical mechanisms contribute to the in-plane mass

flux. The first term in (2) reflects the average particle drift due to the gradient of magnitude of high-frequency oscillations. On average, particles try to “escape” from regions of large fluctuations, the effect analogous to formation of so called Chladni figures [12]. The second term describes diffusive relaxation of the inhomogeneous mass distribution. We expect the effective “granular temperature” and corresponding diffusion constant  $\beta$  to be proportional to the energy of plate vibrations, then for non-vibrating plate the diffusion constant turns to zero and an arbitrary pattern “freezes”.

Let us briefly discuss the linear stability properties of Eqs. (1-2). The trivial state  $\psi = 0$ ,  $\rho = \rho_0$  corresponding to a flat layer oscillating at the driving frequency  $\Omega$  becomes unstable at  $\gamma^2 = \gamma_c^2 = (\omega + b(1 + \rho_0))^2 / (1 + b^2)$  for  $\omega b > 1 + \rho_0$  with respect to a periodic perturbation with the wavenumber  $k_c$  given by  $k_c^2 = (\omega b - 1 - \rho_0) / (1 + b^2)$ . For  $\omega b < 1 + \rho_0$  spatially uniform perturbations with  $k_c = 0$  become unstable first and the vibration threshold is  $\gamma_c^2 = 1 + \rho + \omega^2$ . Due to the rotational invariance of (1-2), waves with all directions grow simultaneously.

Above the threshold, the nonlinear terms in Eqs.(1-2) saturate the exponential growth of perturbations and provide pattern selection. The problem of pattern selection requires careful analysis of patterns with different symmetries. For  $\rho = \text{const}$  Eqs. (1-2) reduce to a single equation for which it is known that rolls are the only stable cellular pattern above onset [13]. This has been a serious shortcoming of this model since square patterns are frequently observed in Faraday experiments [5,11]. Usually pattern selection depends sensitively on the choice of nonlinearity in the model, and some tweaking with non-local nonlinearities could remedy this problem (see e.g. [15]). It turns out that within our combined model with  $\rho$  being a dynamical variable it is not needed, squares and rolls emerge naturally in different parameter regions.

Consider stability of simplest cellular patterns (rolls and squares) in the framework of Eqs. (1-2) close to the threshold of parametric instability. Although the analysis is formally valid for arbitrary rhombic pattern, we restrict ourself by the squares since they are typically preferred by the symmetry. Within the framework of weakly-nonlinear analysis (small supercriticality  $\varepsilon$  defined below) cellular patterns are described by the following solution to Eq. (1):

$$\psi = (A \sin(k_c x) + B \sin(k_c y)) e^{i\phi} + w \quad (3)$$

where  $A(t), B(t)$  are the real amplitudes of two (orthogonal) standing waves, phase  $\phi = \text{const}$  is given by solution of linearized problem, and  $w$  is a correction to the solution which we demand to be small at  $\varepsilon \rightarrow 0$ . Near the threshold the density  $\rho$  is enslaved to  $|\psi|^2$ , and follows the quasi-stationary solution of Eq. (2)  $\rho = \rho_0(t) \exp[-\eta|\psi|^2]$ ,  $\eta = \alpha/\beta$ . The function  $\rho_0(t)$  can be found from the condition of total mass conservation  $S^{-1} \int \rho dx dy = \mu = \text{const}$ ,  $S$  is the total area.

Substituting  $\rho$  into Eq. (1) and performing standard orthogonalization procedure to keep  $w$  small, we obtain the following equations for  $A(t), B(t)$  (for simplicity we retain nonlinearity only in two first orders)

$$\dot{A} = A \left[ \varepsilon + \frac{\mu\eta - 3}{4} A^2 + \frac{2\mu\eta - 3}{2} B^2 - \frac{\mu\eta^2}{2} (B^2 A^2 + 2B^4) \right] \quad (4)$$

Equation for  $B(t)$  is obtained by the permutation  $A \leftrightarrow B$ . The supercriticality parameter is given by  $\varepsilon = \gamma_c(\gamma - \gamma_c) / (1 + \mu + k_c^2)$ . [16]. It follows from Eq.(4) that hysteretic transition to squares ( $A = B$ ) occurs if  $\mu\eta > 9/5$  and stripes ( $A \neq 0, B = 0$  or  $A = 0, B \neq 0$ ) exhibit subcritical bifurcation at  $\mu\eta > 3$ .

In the supercritical case we can drop last two terms in Eq.(4). It is easy to verify that for  $\varepsilon \rightarrow +0$  the square pattern ( $A = B$ ) is stable for  $\mu\eta > 1$  and unstable otherwise. Rolls, in the limit  $\varepsilon \rightarrow +0$ , are stable for  $\mu\eta < 1$  and unstable otherwise. For larger  $\varepsilon > 0$  the higher order terms in Eq. (4) become important, and squares are stable at  $16\mu\varepsilon\eta^2 < 3(10\varepsilon\eta - \varepsilon^2\eta^2 - 9)$  and rolls are stable at  $4\mu\varepsilon\eta^2 > 3(\varepsilon\eta - \varepsilon^2\eta^2 - 3)$ . In the subcritical case  $\eta\mu > 9/5$  squares are stable in their entire basin of existence given by the condition  $48\mu\varepsilon\eta^2 + (5\eta\mu - 9)^2 = 0$ . The phase diagram for roll and squares is shown in Fig. 1. It is qualitatively consistent with the experimental observations of transition from rolls to squares with decreasing the driving frequency if one assumes that  $\eta\mu$  decreases with increase of frequency. One expects that the relative effect of particle drift from regions of intense fluctuations characterized by parameter  $\eta$  diminishes with the increase of  $\omega$  since characteristic vertical scale of the layer involved in oscillations becomes smaller at high frequencies. At large positive  $\varepsilon$  there is a bistable region where rolls and squares co-exist, also in agreement with experiments [5]). It should be noted however, that the phase diagram of Eq.(4) exactly corresponds to the original model (1-2) only in the limit of small amplitude, otherwise it represents only a Galerkin approximation of the exact solution. Still, our numerical simulations agreed fairly well with these stability limits.

Now we consider the localized solutions. In experiments [6] oscillons appear slightly below the threshold of the parametric instability for cellular patterns. We also found stationary localized axisymmetric solutions to Eqs. (1-2) in weakly subcritical region (dots in Fig. 1 correspond to stable localized solutions found for various combinations of parameters). Fig. 2 shows the radial structure of the order parameter  $\psi$  and corresponding distribution of  $\rho$  for such solution. This solution corresponds to a dip in the average mass distribution  $\rho = \rho_0 \exp(-\eta|\psi|^2)$ . Due to the symmetry  $\psi \rightarrow -\psi$ , oscillons of opposite polarities may coexist in this system. It has oscillating tails at  $r \gg 1$ ,  $\psi(r) \propto r^{-1/2} \exp(pr)$  with the (complex) exponent  $p$  given by  $p^2 = -k_c^2 + \sqrt{(\gamma^2 - \gamma_c^2) / (1 + b^2)}$ . It explains

that peaks and craters with elevated periphery replace each other on consecutive cycles of plate vibrations.

We studied the linear stability of these localized solution with respect to axisymmetric (usually the most dangerous) perturbations. Some of the results are presented in Fig. 3, where we show largest eigenvalue of linearized system  $\lambda$ ,  $|\psi(0)|$  and the mass deficit  $m = 2\pi\rho_0(\int_0^\infty r \exp[-\eta|\psi|^2]dr - 1)$ . The stability region is limited both at large and small  $\gamma$  in accord with experiments. At the edges of the stable region,  $\gamma_{c1,2}$ , stable solution corresponding to the oscillon annihilates with other unstable localized solutions.

The interaction of two oscillons can be considered in the spirit of Ref. [17]. Since the asymptotic behavior of  $\psi$  for the oscillon is oscillatory, the interaction force  $F \sim \text{Re} \exp(pr)$  is oscillatory, too. It is natural to expect a variety of bound states. A numerically found bound states of two oscillons with opposite phases is shown in Fig.4a, and a bound state of four oscillons (one positive surrounded by three negative) is shown in Fig.4b. As in the experiment [6] we found that bound states with coordination numbers higher than three are unstable. There also exist a stable bound state of two like-phased oscillons, but the equilibrium distance between the oscillons is substantially larger than for oppositely-phased pairs, resulting in much weaker binding. Small “granular noise” probably unbinds such weakly coupled pairs.

We studied the nonlinear evolution of oscillons beyond their region of stability in numerical simulations of Eq. (1-2). Once the lower bound  $\gamma_{c1}$  is passed, the oscillon rapidly decays towards a trivial state  $\psi = 0$ . Increasing  $\gamma$  above  $\gamma_{c2}$  initial spreading lead to a range of different scenarios depending on other parameters  $\eta, \mu, \omega, \alpha$ . For small  $\eta\mu$  (supercritical transition) oscillons produce a sequence of concentric rolls. Depending on  $\eta\mu$  they either remain rolls or break to produce a disordered square pattern. At larger  $\eta\mu$  oscillon produces other oscillons on its periphery as seen in experiments [6]. It turns out, surprisingly, that following oscillons do not appear uniformly around the center but rather organize themselves in chains, resembling worm-like patterns (Fig.4c), cf. photo by P. Umbanhowar published in [1]. We propose explanation of this effect by the conservation of total mass. Oscillons push the granular material on their periphery. Since the excessive mass from oscillons in a chain is re-distributed by the diffusion, it spreads more rapidly near the tip of the chain. Therefore, the next oscillon will likely appear there, and the tip advances (compare with diffusion-limited growth [18]). This process will continue until the average density in the surrounding flat regions becomes so high that the creation of new oscillons is halted (the threshold for oscillon stability  $\gamma_{c2}$  increases with the average density). Our simulations show that for values of  $\gamma$  slightly above  $\gamma_{c2}$  even after a long time, oscillons do not fill entire area (see Fig. 4d).

Let us now return briefly to the problem of selection

of cellular patterns. In the domain of oscillon stability these patterns can be considered as a periodic lattice of weakly-coupled oscillons. As it is well-known from the solid-state physics, the lowest energy configuration of like-charged objects is a hexagonal lattice (compare with Abrikosov lattice). In contrast, for alternatively-charged particles the optimal configuration is a square lattice where a positively-charged particle is surrounded by four negatively-charged (anti-ferromagnetic lattice). Eqs. (1-2) preserve the symmetry  $\psi \rightarrow -\psi$  and therefore square patterns formed by both positive and negative oscillons dominates (see Fig.4d). Once this symmetry is broken (as in two frequency driving), patterns are formed by like-phased oscillons, and the hexagonal symmetry can be expected. The selection of the pattern in supercritical case where oscillons are unstable is more subtle. The advantage of the square pattern over rhombi cannot be determined in the lowest order of our weakly-nonlinear perturbation theory, which happens to be insensitive to the angle between two standing waves. Our arguments related to optimal packing of localized structures suggests that the unique selection of square patterns should occur in higher orders of  $\varepsilon$ .

We have shown on the basis of phenomenological model that the constraint of mass conservation plays a crucial role in pattern formation in vibrated granular materials. It leads to a subcritical bifurcation towards planar cellular patterns which naturally include squares in a wide range of parameters. The model also reproduces stable localized particle-like excitations (oscillons) and chains of oscillons or short rolls sometimes called worms. The parameters of the model can be estimated experimentally or from molecular dynamics. We can speculate that our results are also relevant for fluids, where square patterns are ubiquitous and localized objects were observed recently [19]. Parametric waves on a fluid surface induce mean surface displacement which must obey a conservation law. Thus, we expect that a coupled set of equations for the order parameter and a mean displacement may serve as a paradigm model for this system. Although for fluids the knowledge of the Navier-Stokes equations allows for the direct stability analysis of cellular patterns [20], finding a relevant order-parameter model would be useful for studies of more complicated pattern formation in this rich experimental system. Worm-like structures have also been recently observed in electroconvection [21]. It is plausible to assume that as in a granular system, this effect can also be interpreted as the growth in a system exhibiting a first-order transition to a cellular structure and controlled by a slowly diffusing field.

We thank M.I.Rabinovich, M.Mungan, H.L.Swinney, P. Umbanhowar and H.Levine for illuminating discussions. This work was supported by the U.S. Department of Energy under contracts DE-FG03-96ER14592 (LT) and W-31-109-ENG-38 (IA). The work of IA was also supported by NSF, Office of Science and Technology

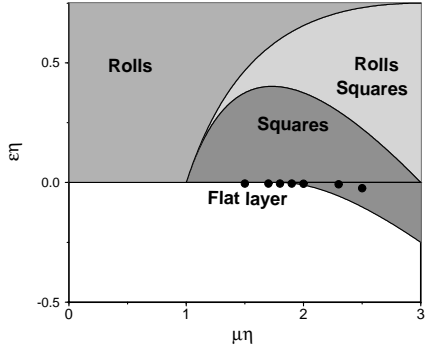


FIG. 1. Phase diagram for square and roll patterns, weakly-nonlinear theory. Black dots indicate stable oscillons seen in numerical experiments

- 
- [1] H.M. Jaeger, S. R. Nagel, and R.P. Behringer, *Rev. Mod. Phys.* **68** (1996).
- [2] I. Goldhirsh and G. Zanetti, *Phys. Rev. Lett.* **70**, 1619 (1993); F. Spahn et al, *Phys. Rev. Lett.* **78**, 1596 (1997); A. Kudrolli, M. Wolpert, and J. Gollub, *Phys. Rev. Lett.* **78**, 1383 (1997); S. McNamara and W.R. Young, *Phys. Rev. E* **50** R28 (1994); Y. Du, L. Hao, and L.P. Kadanoff, *Phys. Rev. Lett.* **74**, 1268 (1995).
- [3] S. N. Coppersmith, et al, *Phys. Rev. E* **53**, 4673 (1996); F. Radjai et. al, *Phys. Rev. Lett.* **77** 274 (1996).
- [4] J. B. Knight, H. M. Jaeger and S. R. Nagel, *Phys. Rev. Lett.* **70**, 3728 (1993).
- [5] F. Melo, P. Umbanhowar and H.L. Swinney, *Phys. Rev. Lett.* **72**, 172 (1994); *ibid* **75**, 3838 (1995).
- [6] P. Umbanhowar, F. Melo and H.L. Swinney, *Nature*, **382**, 793 (1996).
- [7] E.Clement et. al., *Phys. Rev. E* , **53**, 2972 (1996).
- [8] G.H. Ristow and H.J. Herrmann, *Phys. Rev. E* **50**, R5 (1994)
- [9] S. Luding, et al, *Europhys. Lett.* **36**, 247 (1996); K. M. Aoki and T. Akiyama, *Phys. Rev. Lett.* **77**, 4166 (1996).
- [10] M.Faraday, *Phil. Trans. R. Soc. London*, **52**, 299 (1831).
- [11] See, e.g., A.B.Ezersky et al., *Sov.Phys. - JETP*, **64** 1228 (1986); N.B.Tufillaro, R.Ramshankar, and J.P.Gollub, *Phys. Rev. Lett.* , **62**, 422 (1989); S.Ciliberto, S.Douady, and S.Fauve, *Europhys. Lett.*, **15**, 23 (1991).
- [12] The difference is that Chladni figures occur due to non-uniform external vibrations, and here the non-uniformity of oscillations is dynamical.
- [13] W.Zhang and J.Vinals, *Phys. Rev. Lett.* , **74**, 690 (1995).
- [14] S.V.Kiyashko et al., *Phys. Rev. E* , **54**, 5037 (1996).
- [15] M. Cross and P.C. Hohenberg, *Rev. Mod. Phys.* **65** 851 (1993)
- [16] Note that there are other  $O(A^5, B^5)$  terms in Eq. (4) which come from the coupling of the primary waves with their high-order harmonics. However, these terms are small for high internal friction ( $\mu \ll 1$ ,  $\eta \gg 1$ ).
- [17] I.S Aranson et al, *Physica D* **43**, 436 (1990)
- [18] Eqs. (1-2) are reminiscent of phase-field models of dendrite growth, see e.g. J.S.Langer, *Models of Pattern For-*

*mation in First-Order Phase Transitions* (World Scientific, Singapore, 1986).

- [19] O. Lioubashevsky, H. Arbell and J. Fineberg, *Phys. Rev. Lett.* **76**, 3959 (1996).
- [20] P.Chen and J.Viñals, submitted (patt-sol/9702002).
- [21] M.Dennin, G.Ahlers, and D.S.Cannell, *Science*, **272**, 388 (1996).

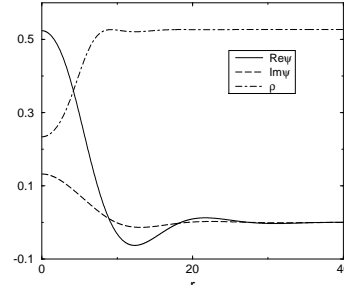


FIG. 2. Radial structure of the stable oscillon for  $\gamma = 1.8$ ,  $\mu = 0.527$ ,  $b = 2$ ,  $\omega = \alpha = 1$ ,  $\eta = 2.78$

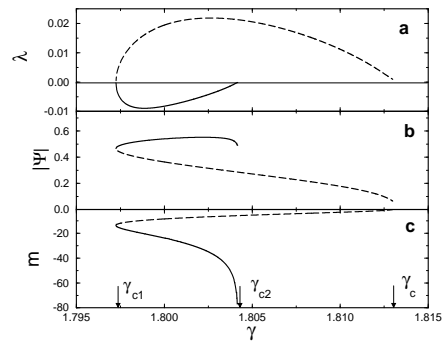


FIG. 3. Largest eigenvalue  $\lambda$  (a),  $|\psi|$  at  $r = 0$  (b) and mass deficit  $m$  (c) for stable (solid line) and unstable (dashed line) oscillons,  $\mu = 0.527$ ,  $b = 2$ ,  $\omega = \alpha = 1$ ,  $\eta = 5/\gamma$ .

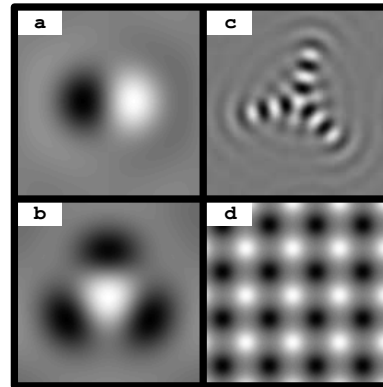


FIG. 4. Gray-coded images of  $\text{Re}\psi$  (black corresponds to maximum, white to minimum) from simulations of Eqs. (1-2), (a) bound state of oppositely-phased oscillons,  $\alpha = \omega = 1, b = 2, \eta = 2.78, \mu = 0.527, \gamma = 1.8$ , size  $L = 40$ ; (b) Triangular bound state, same parameters; (c) worm-like structure produced by a single oscillon in the center,  $\alpha = 1$ ,  $\omega = b = 2$ ,  $\gamma = 2.245, \eta = 4.38, \mu = 0.525$ ,  $L = 100$ ; (d) square lattice,  $\omega = \alpha = 1$ ,  $\gamma = 1.84$ ,  $\mu = 0.52$ ,  $\eta = 2.72$ ,  $L = 100$ .